A FULLY STERILE, COST-EFFECTIVE, RAPIDLY ASSEMBLED, 3D PRINTER FOR BIOPRINTING OF ELECTROGENIC CELL CONSTRUCTS TO DEFINE FUNCTIONAL LAYERS AND ENHANCE SENSITIVITY OF CELL-BASED BIOSENSORS

Cacie Hart, Frank Sommerhage, and Swaminathan Rajaraman
University of Central Florida, Orlando, FL, USA

ABSTRACT

Here we present the conversion of an "off-the-shelf", cost-effective Fused Deposition Modelling (FDM) 3D printer to a fully functional and sterile bioprinter. Additionally, we have developed 3D printed micro-nozzles and compared the bioprinting capabilities of the micro-nozzles to that of standard hand plating, as well as bioprinting thorough a syringe needle. In order to characterize the bioprinting capabilities of the newly developed printer, cardiomyocyte HL-1 cells (a commonly used electrogenic cell line) were successfully printed and observed optically for 5 days *in vitro* (DIV). The micro-nozzle-based printing reports superior print quality and smaller confined geometries compared to the other methods suggesting efficient coupling of cells to potential functional biosensors and biomarkers further demonstrated on plasmonic Interdigitated Electrodes (pIDEs) **[1]**.

KEYWORDS

Bioprinting, 3D Printing, Electrogenic Cells, Micro-nozzles, HL-1 cells, Cell-based Biosensors

INTRODUCTION

In extrusion bioprinting, material (bioink and cells) is dispensed through a nozzle (or syringe) using either pneumatic or mechanical pressure (i.e. plunger, screw, etc.). The larger nozzle size of extrusion printers leads to less clogging when compared to inkjet printing **[2]**. This means that the potential to deposit higher densities of cells exists and that a wider range of bioinks with varying viscosities can be used. Extrusion bioprinting is typically a continuous flow process; however, in some cases, discrete spots may be deposited **[3]**.

Commercial extrusion bioprinters are exceedingly expensive (upwards of $200,000); thus, this technique is often overlooked in laboratory settings despite this technology being the most promising of the three major bioprinting technologies for clinical translation **[4]**. Most "hobby" 3D printers are extrusion printers, and these are extremely inexpensive and relatively open source since the original patents for this technology (FDM) expired some time ago. For this reason, there is potential for the cost to greatly decrease and to implement all the advantages of this technique by converting an "off-the-shelf" FDM printer to a bioprinter, similar to what was done for inkjet printing.

In addition to the cost, simplicity and the ability to "Do it Yourself (DIY)", extrusion bioprinting has many advantages over other techniques which can be exploited to define finicky electrogenic or electrically active cellular constructs. Extrusion printing allows for greater deposition and printer speed, which can facilitate scalability in a timely manner **[5]**. Extrusion bioprinting can accommodate a wide variety of bioinks inks including cell aggregates, cell-laden hydrogels, micro-carriers, and decellularized matrix components, while other techniques are only capable of printing cell-laden hydrogels **[6-9]**. Additionally, bioprinting at high cell densities is currently feasible only using extrusion bioprinting. Such a bioprinting process is biocompatible with reasonably small process-induced cell damage and injury compared to other techniques **[10, 11]**. Additionally, it is capable of producing anatomically correct porous constructs, which is challenging with other methods. Most importantly as mentioned earlier, from an implementation perspective, extrusion bioprinting techniques are easy to implement and can be used by those with limited exposure to the technology and laboratories in low-resource settings.

The major disadvantage of extrusion bioprinting is the limited resolution. The minimum feature size is generally well in excess of 100 µm **[10]**. This resolution is considerably lower than other techniques. Inkjet and laser-based bioprinting can achieve resolutions of 50 µm and 5 µm, respectively **[4]**.

Notable work on bioprinting using extrusion techniques has been performed by several groups. Khalil and Sun report on the extrusion bioprinting of 3D hydrogel scaffolds. In this study, rat heart endothelial cells were encapsulated in various hydrogel solutions, including alginate, fibrin, and chitosan, and printed. Their minimum feature sizes were shown to be approximately 250 µm **[12]**. Bertassoni et al. showed direct-write bioprinting of cell-laden methacrylated gelatin hydrogels. This work involved printing HepG2 and NIH3T3 cells suspended in a methacrylated gelatin hydrogel using a commercial extrusion bioprinter (NovoGen MMX Bioprinter). They showed minimum feature sizes of ~ 500 µm and their hydrogels needed ultraviolet exposure to set into defined patterns **[13]**. There has been other work reported in this area as well, however, extrusion bioprinting of "tricky to print and grow" electrically active cell constructs is largely missing from literature.

In this work, we fully convert a commercial "off-the-shelf" FDM printer into a cost-effective and customizable sterile bioprinter. Additionally, we demonstrate printing of electrogenic cells through both a hypodermic needle and a 3D printed micro-nozzle demonstrating reduced size constructs and superior coupling to underlying surfaces. The bioprinting process is compared to traditional hand plating as depicted schematically in **Fig. 1**. Lastly, we depict feasibility of cellular coupling by printing electrogenic cells atop plasmonic Interdigitated Electrodes **[1]**.

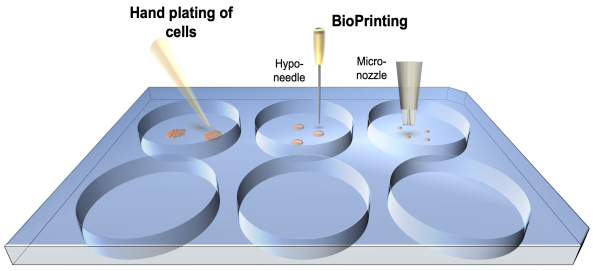

Fig.1*: A broad schematic depicting the hypothesized differences between hand plating (left), hypodermic hollow needle bioprinting (center) and micro-nozzle-based bioprinting in a 6-well plate. The size of the printed dots is expected to reduce as we move to the right.*

MATERIALS AND METHODS

A Tronxy X1 printer was fully assembled inside a biosafety cabinet to ensure sterility from the onset. All components of the

978-1-940470-04-7/HH2022/$25©2022TRF
DOI 10.31438/trf.hh2022.56

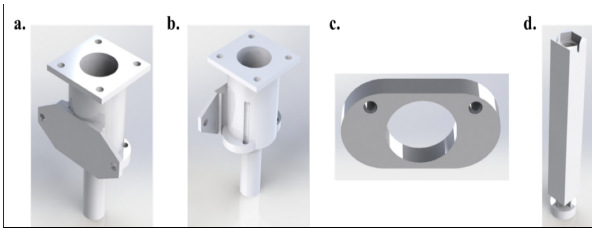

***Fig. 2**: Syringe pump schematics: a. and b. Final syringe pump body design. Designed to fit directly onto the extruder plate of the Tronxy X1; c. Syringe holder designed to keep the syringe fixed to the syringe pump during printing; d. Syringe insert. Designed to fit rubber syringe gasket for improved performance. The M5 hex nut is glued to the insert to ensure perfectly coupled movement.*

printer, as well as tools, were heavily sprayed with 70% isopropyl alcohol prior to introduction into the biosafety cabinet. The sterile environment of the biosafety cabinet needed to be maintained, as well. The purchased polymer extruder was not affixed to the printer, as a custom-built syringe pump was attached in its place.

The syringe pump was designed in SolidWorks and 3D printed on a separate RepRap FDM 3D printer (Tevo Tarantula) in 1.75mm polylactic acid (PLA) plastic in a rectilinear pattern with a 25% infill density at 35 mm/s with an extruder temperature of 200°C and a bed temperature of 60°C. The syringe pump was comprised of three parts: (1) the body (**Fig. 2A and B**), (2) the syringe holder designed to keep the syringe fixed to the syringe pump during printing (**Fig. 2C**), and (3) the syringe inserts (**Fig. 2D**).

In order to demonstrate smaller print sizes two different printing technologies were compared: a commercially purchased 30G hypodermic hollow needle (from BD) and 3D printed micro-nozzles. The latter devices were designed in SolidWorks. Outer nozzle dimensions were designed to a height of 16.4 mm and width of 6.25 mm at the top and 250 µm at the bottom (**Table I**). The inner nozzle dimensions were 4.25 mm top opening with a height of 6.4 mm, followed by a tapered cone area with a height of 5 mm, followed by a cylinder of 1 mm height and 100 µm width, and finally another cone leading to the opening that starts with a width of 100 µm and ends with 250 µm opening and is 500 µm in height. This design is subsequently printed on an Asiga Digital Light Processing (DLP) 3D Printer in High Temperature (FLAMHT01) resin from

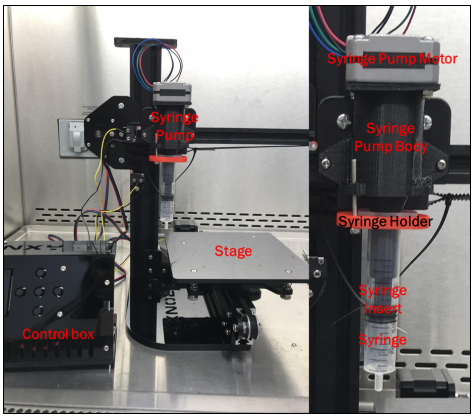

***Fig. 3**: Fully converted Tronxy X1 3D printer inside a biosafety cabinet. Left: wide view showing the entire set-up including the control box, stage, and syringe pump. Right: close-up of the syringe pump.*

FormLabs. After printing, the micro-nozzles were subjected to a

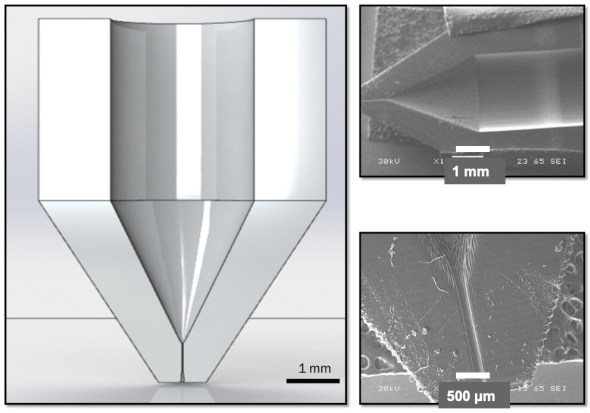

***Fig. 4**: 3D printed micro-nozzle: Left: SolidWorks schematic showing the intended design of the nozzle; Right Top: SEM of the full micro-nozzle; Right Bottom: SEM of the micro-nozzle outlet through which cells are printed/extruded.*

previously developed rigorous post-print treatment in order to ensure biocompatibility with cells **[14].**

Electrogenic cell constructs (HL-1 cells) were printed in a 3% w/v gelatin solution and maintained as previously described **[14, 15]**. Cells were printed using 30G dispensing needles, as well as 3D printed micro-nozzles on separate 6-well plates and pIDE substrates. Additionally, hand plating of cells on a third 6-well plate was used as a control. Cells were grown for 5 days *in vitro* (DIV) and then imaged using confocal microscopy (Keyence BZ-X800). Live/Dead assays was performed at 5DIV using previously reported techniques **[14]** after observation of cells throughout the time period.

RESULTS AND DISCUSSIONS

Extrusion printing of cells was modeled phenomenologically by Nair et al. **[16]**. This model predicts the viability of live cells in extrusion printing as function of nozzle diameter and shear pressure **[16]**. Plugging in the value of the measured 30G needle diameter (~312µm) and the micro-nozzle design diameter (250µm) in test shear pressures provides ***in excess of 90% cellular viability in both cases: 96.21% for hypodermic needle and 91.19% for micro-nozzle*** increasing the confidence of achieving successful results with our bioprinter design.

A Tronxy X1 printer was successfully assembled inside of a biosafety cabinet to ensure sterility from the onset. **Fig. 3** depicts an optical micrograph of the fully assembled printer. The micro-nozzle moves in the x and z directions, while a stage moves in the y direction. This gives the ***user complete special control*** of the cellular deposition process. In addition, ***micro-nozzles were successfully printed*** and post-treated for biocompatibility as depicted in the design and SEM images (**Fig. 4**).

Table I depicts the "gross" and "fine" features of the 3D printed micro-nozzles. The "gross" features printed close to the design value. However, the "fine" features did not have the same result. The cone structure at the bottom of the micro-nozzle could not be resolved. Possible design iterations, print angle variations and material changes are envisioned in future versions of the micro-nozzle to improve design to device of this component.

Initial testing of the converted 3D printer required many test prints. While the focus remained on dot printing due to the nature of the biosensor design (circular microelectrode arrays (MEAs) and pIDEs) and cell coupling to these sensors in our laboratory **[17]**, ***several other patterns were explored and printed***. These patterns can be observed as micrographs in **Fig. 5**. During this phase of the bioprinter characterization process, it was found that blanket coating

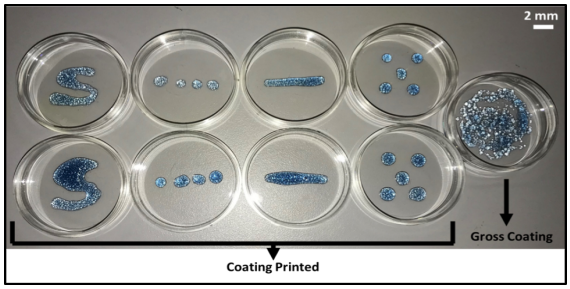

Fig. 5*: Cells were printed in a variety of patterns. Initially, the petri dishes were grossly coated with fibronectin. This resulted in full surface wetting due to the hydrophilic nature of both the petri dish and the fibronectin. To achieve the desired patterns, it was necessary to print the coating, as well. Printed patterns include dots, lines, and an S-shape depicting printing fibronectin followed by bioprinting of HL-1 cell-laden bioink. Scale bar on top is 2mm.*

of the cell plating surface with fibronectin to encourage cells to adhere to the surface caused full surface wetting upon droplet impact due to the hydrophilic nature of both the petri dish and the fibronectin **[18]**.

After these successful initial tests, HL-1 laden bioink was defined on 3 different 6-well plates: hand plating (control), hypodermic needle printing and printing through micro-nozzle. Additionally, test prints were performed on pIDE substrates. In order to compare the bioprinting through the 30G needles and the micro-nozzles with hand plating, the radius of the printed dots was measured throughout 5 DIV prior to the live/dead assay. The hypothesis going in was the 30G and micro-nozzle printing would dramatically reduce the dot sizes and provide the user with better control and coupling of cells to the underlying surface. The ***results followed the expected trends very well over the full assay of five days*** (**Fig. 6**). The hand plated spots were consistently the largest and uncontrolled. They had a radius of 2192 µm ± 111 µm (N=6) when initially plated and grew as expected over the course of the five days. The radius of the hand plated spots grew by 523 µm ± 81 µm over the course of five days. The spots printed with the 30G hollow, hypodermic needle were the "intermediate" sized spots, with their average radius being approximately 1351 µm ± 105 µm

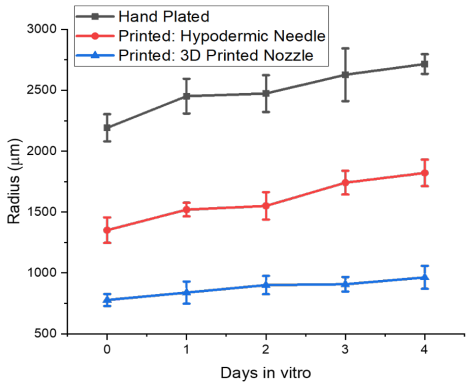

Fig. 6*: Comparison of sizes between spots that were hand plated, bioprinted using a hypodermic needle, and bioprinted using the 3D printed micro-nozzle. The 3D printed micronozzle provides the smallest spot sizes affording best control and cellular coupling to underlying surface.*

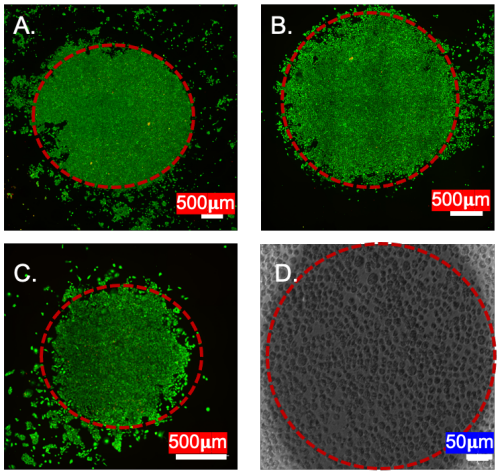

Fig. 7*: Live/Dead example confocal images of the three cell (HL1 cardiomyocytes) plating conditions at 5DIV and cells on pIDE biosensors [1]- A: hand plated; B: bioprinted using a hypodermic needle; C: bioprinted using the 3D printed micro-nozzle; and D: on plasmonic IDE sensors. All four conditions showed similar, excellent viability at 5DIV.*

(N=6) when printed and grew as expected over the course of the five days. The radius of the spots printed with the hypodermic needle grew by 470 µm ± 56 µm. Finally, the spots printed with the 3D printed micro-nozzle were the ***smallest of the three*** with their radius being approximately 775 µm ± 49 µm (N=6) when initially printed. They also grew as expected over the course of the five days. The radius of the spots printed with the 3D printed micro-nozzles grew by 188 µm ± 24 µm over the course of the five days. All three bioprinting conditions demonstrated ***excellent viability*** (**Fig. 7A-C**) in the live/dead assay at 5DIV. Additionally, the ***sensitivity of pIDEs can further be enhanced with superior coupling*** with printed electrogenic cells and the first steps towards this sensitivity enhancement were demonstrated (**Fig. 7D**).

CONCLUSIONS

The converted Tronxy X1 3D printer provides an excellent "do-it-yourself" solution for electrogenic cell bioprinting. Although the lowest achieved resolution is approximately 725 µm and can be improved in future experiments, it still provides better cell-electrode coupling when compared to hand plating on a biosensor device in addition to improving specificity and reducing costs of cell culture. This resolution can be improved with higher resolution micro-nozzles and improved 3D printed designs of these structures.

Table I: Design and Measured Dimensions of the Micro-Nozzle

Dimension	***Design Value***	***Measured Value***
Nozzle Height	*16.4mm*	*~16.4mm*
Top Nozzle Width	*6.25mm*	*~6.24mm*
Bottom Nozzle Width	*250µm*	*150 µm+/-11 µm*
Inner Nozzle Cone Opening	*4.25mm*	*~4.25mm*
Inner Nozzle Cone Height	*6.4mm*	*~6.4mm*
Cylinder Height	*1mm*	*1.5mm*
Cylinder Width	*100 µm*	*150 µm+/-11 µm*
Cone Height	*500 µm*	*Did not define*
Cone Width	*250 µm*	*Did not define*

Feasibility towards coupling these printed cells with biosensors such as plasmonic IDEs were further demonstrated. Moving forward such a technique will be invaluable to emerging areas such as personalized medicine, “clinical trials on a chip” and “patient-on-a-chip” technologies.

ACKNOWLEDGEMENTS

This work was supported by the University of Central Florida both from start-up funding of the PI (Prof. Rajaraman) and a doctoral support award for Ph.D. thesis completion (Ms. Hart).

REFERENCES

[1] C. Hart, K. Kumar, J. Li, J. Thomas, and S. Rajaraman, IEEE JMEMS, vol. 29, no. 5, pp. 1109 – 1111, 2020.

[2] J. He, X. Zhao, J. Chang, and D. Li, "Microscale Electro-Hydrodynamic Cell Printing with High Viability," Small, vol. 13, no. 47, p. 1702626, 2017, doi: 10.1002/smll.201702626.

[3] G. Gao, Y. Huang, A. F. Schilling, K. Hubbell, and X. Cui, "Organ Bioprinting: Are We There Yet?," Advanced Healthcare Materials, vol. 7, no. 1, p. 1701018, 2018, doi: 10.1002/adhm.201701018.

[4] J. Jang, J. Y. Park, G. Gao, and D.-W. Cho, "Biomaterials-based 3D cell printing for next-generation therapeutics and diagnostics," Biomaterials, vol. 156, pp. 88-106, 2018/02/01/ 2018, doi: https://doi.org/10.1016/j.biomaterials.2017.11.030.

[5] I. T. Ozbolat and M. Hospodiuk, "Current advances and future perspectives in extrusion-based bioprinting," Biomaterials, vol. 76, pp. 321-343, 2016/01/01/ 2016, doi: https://doi.org/10.1016/j.biomaterials.2015.10.076.

[6] T. Boland, V. Mironov, A. Gutowska, E. A. Roth, and R. R. Markwald, "Cell and organ printing 2: Fusion of cell aggregates in three-dimensional gels," The Anatomical Record Part A: Discoveries in Molecular, Cellular, and Evolutionary Biology, vol. 272A, no. 2, pp. 497-502, 2003, doi: 10.1002/ar.a.10059.

[7] V. Mironov, R. P. Visconti, V. Kasyanov, G. Forgacs, C. J. Drake, and R. R. Markwald, "Organ printing: Tissue spheroids as building blocks," Biomaterials, vol. 30, no. 12, pp. 2164-2174, 2009/04/01/ 2009, doi: https://doi.org/10.1016/j.biomaterials.2008.12.084.

[8] J. Malda et al., "25th Anniversary Article: Engineering Hydrogels for Biofabrication," Advanced Materials, vol. 25, no. 36, pp. 5011-5028, 2013, doi: 10.1002/adma.201302042.

[9] R. Levato, J. Visser, J. A. Planell, E. Engel, J. Malda, and M. A. Mateos-Timoneda, "Biofabrication of tissue constructs by 3D bioprinting of cell-laden microcarriers," Biofabrication, vol. 6, no. 3, p. 035020, 2014/07/22 2014, doi: 10.1088/1758-5082/6/3/035020.

[10] B. Duan, L. A. Hockaday, K. H. Kang, and J. T. Butcher, "3D Bioprinting of heterogeneous aortic valve conduits with alginate/gelatin hydrogels," Journal of Biomedical Materials Research Part A, vol. 101A, no. 5, pp. 1255-1264, 2013, doi: 10.1002/jbm.a.34420.

[11] S. Boularaoui, G. Al Hussein, K. A. Khan, N. Christoforou, and C. Stefanini, "An overview of extrusion-based bioprinting with a focus on induced shear stress and its effect on cell viability," Bioprinting, vol. 20, p. e00093, 2020/12/01/ 2020, doi: https://doi.org/10.1016/j.bprint.2020.e00093.

[12] S. Khalil and W. Sun, "Biopolymer deposition for freeform fabrication of hydrogel tissue constructs," Materials Science and Engineering: C, vol. 27, no. 3, pp. 469-478, 2007/04/01/ 2007, doi: https://doi.org/10.1016/j.msec.2006.05.023.

[13] L. E. Bertassoni et al., "Direct-write bioprinting of cell-laden methacrylated gelatin hydrogels," Biofabrication, vol. 6, no. 2, p. 024105, 2014/04/03 2014, doi: 10.1088/1758-5082/6/2/024105.

[14] C. Hart, C. M. Didier, F. Sommerhage, and S. Rajaraman, "Biocompatibility of Blank, Post-Processed and Coated 3D Printed Resin Structures with Electrogenic Cells," Biosensors, vol. 10, no. 11, p. 152, 2020. Available: https://www.mdpi.com/2079-6374/10/11/152.

[15] W. C. Claycomb et al., "HL-1 cells: A cardiac muscle cell line that contracts and retains phenotypic characteristics of the adult cardiomyocyte," Proceedings of the National Academy of Sciences, vol. 95, no. 6, pp. 2979-2984, 1998, doi: 10.1073/pnas.95.6.2979.

[16] K. Nair et al., "Characterization of cell viability during bioprinting processes," Biotechnology Journal, vol. 4, no. 8, pp. 1168-1177, 2009, doi: 10.1002/biot.200900004.

[17] N. Azim et al., “Precision Plating of Human Electrogenic Cells on Microelectrodes Enhanced with Precision Electrodeposited Nano-Porous Platinum for Cell-Based Biosensing Applications,” IEEE JMEMS, 28 (1), pp. 50-62, (2019).

[18] F. Grinnell and M. K. Feld, "Fibronectin adsorption on hydrophilic and hydrophobic surfaces detected by antibody binding and analyzed during cell adhesion in serum-containing medium," (in eng), J Biol Chem, vol. 257, no. 9, pp. 4888-93, May 10, 1982.

CONTACT

*Swaminathan Rajaraman, tel: +1-407-823-4339; Swaminathan.Rajaraman@ucf.edu